Compact multiband left-handed metamaterial at terahertz frequencies

Qiujiao Du (杜秋姣)[1,2], Jinsong Liu (刘劲松)[1*], and Hongwu Yang (杨洪武)[3]

[1] *Wuhan National Laboratory for Optoelectronics, School of Optoelectronic Science and Engineering, Huazhong University of Science and Technology, Wuhan 430074, China*

[2] *School of Mathematics and Physics, China University of Geosciences, Wuhan 430074, China*

[3] *School of Civil Engineering and Mechanics, Huazhong University of Science and Technology, Wuhan 430074, China*

[*] *Corresponding author: jsliu4508@vip.sina.com*

Received July 4, 2011; accepted August 15, 2011; posted online October 24, 2011

We design and analyze a novel multiband left-handed metamaterial based on a fishnet-like structure at terahertz (THz) frequencies. The metamaterial exhibits simultaneous negative refractions around the frequencies of 0.48, 1.05, and 1.19 THz for the electromagnetic (EM) wave normal incidence, and around the frequencies of 0.20, 0.79, and 1.13 THz for parallel incidence. The simulated results verify the left-handed properties. A particularly important observation is the capability of the proposed metamaterial with a single geometrical structure to display multifrequency operations in a unit cell. The compact metamaterial is a major step toward the miniaturization of THz materials and devices suitable for multifrequencies.

OCIS codes: 160.3918, 300.6495, 350.3618.

doi: 10.3788/COL201109.110015.

Teraherz (THz) science and technology field has attracted significant attention due to its potential applications in security checking, biomedical imaging, and wireless communication, among others. However, the development of THz technology has been relatively slow and mainly affected by the lack of natural materials with useful responses in this regime[1]. Moreover, THz radiation occupies part of the electromagnetic (EM) spectrum between the microwave and infrared waves, where both the electric and photonic responses of materials die out.

Metamaterials are a new class of composite artificial materials, which in contrast to other composite materials, acquire their properties from an internal structure. In the THz regime, metamaterials provide an optimistic approach to overcoming the limitations of natural materials in the construction of novel functional THz devices[2−4]. In recent years, ample proof of the existence of left-handed metamaterials (LHMs) in the microwave frequency regime has been presented. The first LHM in the world[5] was constructed by arranging the arrays of split ring resonators (SRRs) and wires alternately. A wide variety of LHMs have been designed and fabricated, such as the Ω-shaped model[6], S-shaped model[7], H-shaped model[8], short wire pair[9], and fishnet structure[10]. Researchers have been striving to push the operating frequency of LHMs into the THz and optical regimes. However, most of the LHMs are only applicable to a narrow frequency range due to the nature of the resonator. Considering the practical applications of the LHMs, the realization of broadband has become the main subject of LHM research. Thus far, there have been several reports on the realization of multiband LHMs with different geometrical structures in a unit cell[11,12]. In the gigahertz (GHz) range, no difficulty is encountered in fabricating these multiband metamaterials. However, at high frequencies, it is difficult to print multiple structures on the substrate.

In this letter, we propose a THz fishnet-like metamaterial with a single geometrical structure in a unit cell, from which multiple left-handed bands have been found. Numerical simulations proved that left-handed multiple bands can be gained for THz wave either normal or parallel incidence to the surface of the structure. In particular, owing to the characteristics of simple fabrication and compact structure, the possibility of fabricating small THz devices suitable for multifrequencies exists.

We combine two perpendicular pairs of metallic plates and metallic cross wires with different sizes into a fishnet-like structure cell, as shown in Fig. 1. The metamaterial cell arrays are in the x and y directions, with lattice constants of 150 and 150 μm. A unit cell of the metamaterial is obtained using a commercial finite element-based electromagnetic field solver. Figure 1 shows the orthogonal plate structure. The dimensions of the large plate pairs are 100×130 (μm), and those of the small plate pairs are 130×40 (μm). The metal layer is 400-nm thick. In the

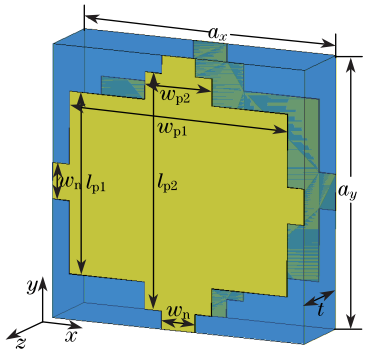

Fig. 1. (Color online) Schematic of the fishnet-like structure with geometric parameters: $a_x = a_y = 150$ μm, $l_{p1} = 100$ μm, $l_{p2} = w_{p1} = 130$ μm, $w_{p2} = 40$ μm, $w_n = 20$ μm, and $t = 40$ μm. The structure consists of patterned double metal layers (yellow, gold) separated by a gallium arsenide layer (blue, GaAs).

model, we use gallium arsenide (GaAs) as substrate, which has a moderate dielectric constant $\varepsilon_r = 12.8$ (real part) and a low loss tangent of 0.006 in the THz range. In addition, we choose gold, which is a good conductor, to reduce the losses.

We investigate two cases with electric polarization parallel to the y axis defined in Fig. 1. One is the normal incidence ($\mathbf{k}//z$) and the other is the parallel incidence ($\mathbf{k}//x$). Different mechanisms for the two cases are used to realize the negative refraction in the fishnet-like structure.

For the normal incidence, the mechanism of negative refraction is similar to the regular fishnet structure. The metal cells on opposite sides of the substrate contribute to the magnetic resonance. In addition, the metal cell can show the behavior of the cut wire in the **E** direction, and realize negative permittivity in a particular frequency band[9,10]. Our simulations show that negative permittivity and negative permeability overlapping in the same band can be achieved by adjusting parameters.

We simulate the transmission properties of the fishnet-like metamaterial, as shown in Fig. 2(a). In the simulation, perfect electric and magnetic boundaries are assigned on the transverse surfaces in the y and x directions, respectively, and two waveguide ports are constructed in the z direction. For a complete quantitative characterization of the EM properties of the metamaterial, we apply a retrieval procedure[13,14] to calculate the effective EM parameters from the simulated reflection and transmission data. Based on a two-port network, the complex refractive index n and wave impedance Z are given by

$$n = \frac{1}{kd}\cos^{-1}\left[\frac{1}{2S_{21}}(1 - S_{11}^2 + S_{21}^2)\right], \tag{1}$$

$$Z = \sqrt{\frac{(1+S_{11})^2 - S_{21}^2}{(1-S_{11})^2 - S_{21}^2}}, \tag{2}$$

where S_{11} and S_{21} denote the reflection and transmission coefficients, respectively. Knowing the values of n and Z, we can easily obtain permittivity and permeability by using the simple formula

$$\varepsilon = n/Z, \quad \mu = nZ. \tag{3}$$

The resulting effective parameters, as a function of frequency, are plotted in Fig. 2.

The retrieved index of n in Fig. 2(b) shows three negative index bands around 0.48, 1.05, and 1.19 THz. A negative index band may include the single-negative band and double-negative band[15]. Thus, we show permeability and permittivity as a function of frequency in Figs. 2(c) and (d). Figure 2(c) shows that the metamaterial exhibits three narrow negative permeability bands between 0.47 and 0.5 THz, between 1.05 and 1.08 THz, and between 1.18 and 1.21 THz. Figure 2(d) shows four relatively broad negative permittivity bands below 0.52 THz, between 0.667 and 0.765 THz, between 0.772 and 1.01 THz, and above 1.05 THz. Therefore, the metamaterial exhibits three left-handed bands between 0.47 and 0.5 THz, between 1.05 and 1.08 THz, and between 1.18 and 1.21 THz, where four wide negative electric response bands overlap three narrow negative magnetic response bands.

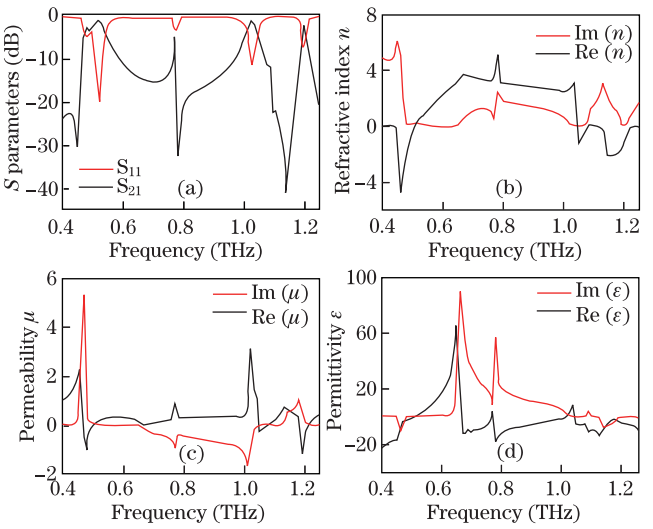

Fig. 2. Magnitude of scattering parameters (S_{11} and S_{12}) and retrieved effective electromagnetic parameters under normal incidence.

Negative permeability is the result of a strong resonance response to an external magnetic field. To illustrate further its magnetic resonance performance, we investigate the current distribution at each magnetic resonance frequency. The surface current distribution at the inner metallic surface of the fishnet-like structure is shown in Fig. 3. From the current distribution, plate pairs of different sizes produce magnetic resonance behaviors at three resonant frequencies. We take the magnetic response at 0.48 THz, for example, to examine the mechanism of negative permeability. In Fig. 3(a), the large plate structure provides the first magnetic resonant response in 0.48 THz, associated with strong antiparallel currents in the two plates and two necks of the pair. The strong currents show a strong magnetic response at the neck parts. These currents are the opposite of those at the plate regions, thereby producing a strong charge accumulation at the regions where the two opposite flowing currents meet[10]. The induced currents in the metallic plates and necks of the opposite sides of the substrate form circular currents and exhibit self-inductance (L). Together with the capacitance (C) between the opposite metallic plates, the fishnet-like structure works like a LC resonant circuit and provides negative permeability. According to the LC circuit theory, the magnetic resonance frequency, ω_m, can be written as $\omega_m^2 = 1/(L_p C_m) + 1/(L_n C_m)$, where the capacitance C_m is given by the simple formula $C_m \propto w_{p1} l_{p1}/t$, the plate inductance $L_p \propto l_{p1} t/w_{p1}$, and the neck inductance $L_n \propto l_n t/w_n$, where l_n is the length of the necks. We can deduce the magnetic-resonance frequency for the form with

$$f_m = \frac{\omega_m}{2\pi} \propto \sqrt{\frac{1}{l_{p1}^2} + \frac{1}{l_{p1} l_n}\frac{w_n}{w_{p1}}}. \tag{4}$$

From Eq. (4), we find that the magnetic resonance frequency depends on the sizes of the plate and neck in the y direction. Similarly, the other two negative magnetic resonances at 1.05 and 1.19 THz occur in plate pairs of different sizes.

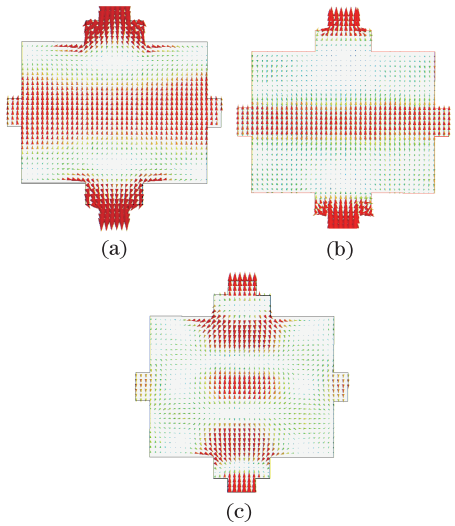

Fig. 3. Surface current distribution under normal incidence at magnetic resonance frequencies of (a) 0.48, (b) 1.05, and (c) 1.19 THz, respectively.

Negative permittivity can be achieved by either plasmonic behavior or resonance to the external electric field. Figure 2(d) shows that the metamaterial exhibits four wide negative permittivity bands. The first negative permittivity band in the lower frequencies is excited by a plasmonic behavior of wires due to the interconnected topology of the metal wires. The plasma frequency $\omega_{\rm p} = 0.52$ THz can be tailored by specifying the distance between the wires, and the sizes of their cross sections[16]. However, the electric response in the higher frequencies is not determined by the Dude-like response of the wires. We have to take into account the dipole-like electric resonant response of the plate pair structure producing the magnetic response. Considering the effective LC circuit description close to the electric resonance frequency[10], the electric-resonance frequency is given by

$$f_{\rm e} = \frac{\omega_{\rm e}}{2\pi} \propto \sqrt{\frac{1}{w_{\rm p1}\ln(l_{\rm p1}/w_{\rm p1})} + \frac{1}{w_{\rm p1}\ln(l_{\rm n}/w_{\rm n})}}. \quad (5)$$

The plate pair electric resonance frequency depends on the length $l_{\rm p1}$ and width $w_{\rm p1}$ of the plates. Hence, the other three negative permittivity bands are provided by the electric response of plate pairs with different sizes.

For parallel incidence, the mechanism of negative refraction is similar to the SRR and wire structure. In the simulation, the electric and magnetic fields are polarized along the y and z directions, respectively. Under this polarization, we simulate the transmission response of the fishnet-like structure unit with the wave vector along the x direction and obtain the effective EM parameters from the simulated S parameters.

The simulated transmission and reflection results are plotted in Fig. 4(a). From the power transmittance, we find that the metamaterial exhibits four pass bands. However, we are uncertain if these pass bands are left-handed bands. To verify the left-handed behavior of the metamaterial, the effective EM parameters are derived from the S parameters according to Eqs. (1), (2), and (3). The results are presented in Fig. 4. The plots show that the permittivity, permeability, and refractive indexes are all negative over a band between 0.19 and 0.30 THz. Thus, the bands are verified as left-handed bands. Similarly, two other left-handed bands between 0.79 and 0.84 THz, and between 1.11 and 1.14 THz are found.

To understand the magnetic response of the metamaterial to the EM wave for the parallel incidence, the distributions of the current in the metallic plates at three magnetic resonance frequencies are shown in Fig. 5. At the first resonance frequency of 0.19 THz, the magnetic inductive currents at the necks in Fig. 5(a) produce a self-inductance (L) at each neck region, with respect to the magnetic field of the incident EM wave. Furthermore, the charges are accumulated at the four angles of the large plate, and capacitance (C) at each angle region between the neighbor plates in a single metallic layer is produced. The capacitances, together with the inductances, form an LC resonant circuit. Subsequently, the effective circuit exhibits a negative magnetic response.

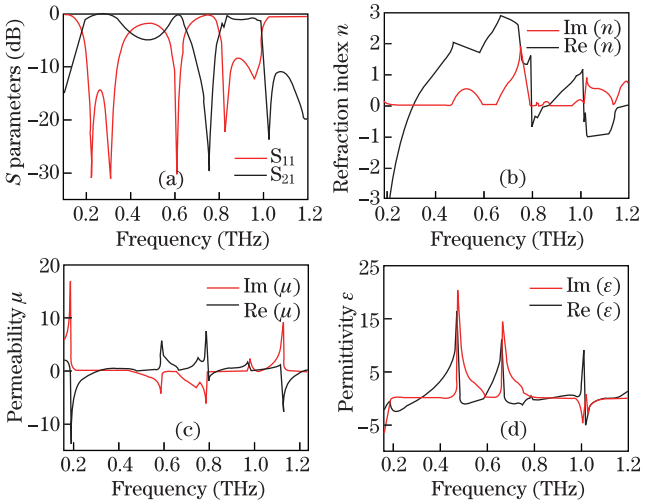

Fig. 4. Magnitude of scattering parameters (S_{11} and S_{21}) and retrieved effective EM parameters under the parallel incidence.

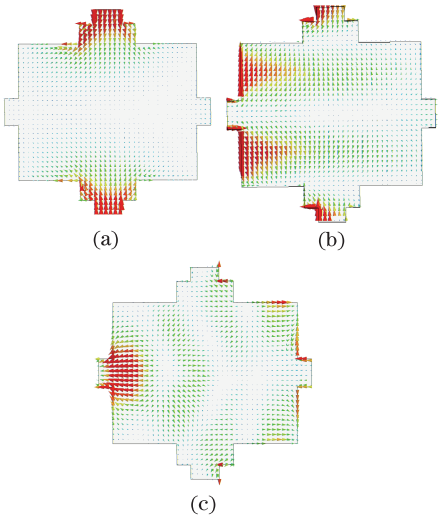

Fig. 5. Surface current distribution under the parallel incidence at magnetic resonance frequencies of (a) 0.19, (b) 0.79, and (c) 1.13 THz, respectively.

The metamaterial provides a negative permeability band around the magnetic resonance frequency of 0.19 THz. The EM behaviors at 0.79 THz are shown in Fig. 5(b). Due to the different charges and current distributions, the effective capacitances and inductances change. The magnetic resonance frequency shifts up to 0.79 THz. Similarly, the EM properties are found at the frequency of 1.13 THz as shown in Fig. 5(c).

For parallel and normal incidences, the electric field of the electromagnetic wave is always parallel to the y axis; hence, the similar electric response for the two cases. The metamaterial exhibits four wide negative permittivity bands. The first negative permittivity band, below 0.31 THz, is excited by the plasmonic behavior of wires due to the equivalent topology of the metal plates and wires. Compared with the electric response ($\omega_{\rm p} = 0.52$ THz) of the wires for the normal incidence, we find that the electric plasma frequency ($\omega_{\rm p} = 0.31$ THz) for the parallel incidence shows an evident red shift by 0.21 THz. The shift is due to the variations in the induced current distribution in the metallic plates and wires. However, the electric response in the higher frequencies is determined by the resonant dipole-like electric response of the plate pair structures. Based on the effective LC circuit description close to the electric resonance frequency, we realize that the plate pair electric resonance frequency depends on the size of the plate pair. The other three negative permittivity bands around 0.51, 0.76, and 1.08 THz are provided by the electric resonant response of plate pairs with different sizes.

In conclusion, we demonstrate a compact multiband left-hand metamaterial operating in the THz frequency range. Its left-handed behaviors are studied through numerical simulations. Under the condition that THz wave propagates normally to the surface, the metamaterial achieves left-handed characteristics around 0.48, 1.05, and 1.19 THz, simultaneously. Under the condition that THz wave propagates parallel to the surface, the metamaterial achieves left-handed characteristics around 0.20, 0.79, and 1.13 THz, simultaneously. Lastly, this simple planar metamaterial can be easily extended to the three-dimensional metamaterial through layer by layer stacking. Therefore, the metamaterial offers a wide variety of applications in the THz frequency range, such as wave plate, band pass filters, and beam steerers, among others. With regard to possible wider applications, the operating frequency of the metamaterial can be adjusted by modifying the structure design.

This work was supported by the National Natural Science Foundation of China (Nos. 10974063 and 10876010) and the Foundation Research Funds for the Central Universities (No. 2010MS041).

References

1. B. Ferguson and X. C. Zhang, Nature Mater. **1,** 26 (2002).
2. H. T. Chen, W. J. Padilla, J. M. O. Zide, A. C. Gossard, A. J. Taylor, and R. D. Averitt, Nature **444,** 597 (2006).
3. H. T. Chen, H. Lu, A. K. Azad, R. D. Averitt, A. C. Gossard, S. A. Trugman, J. F. O'Hara, and A. J. Taylor, Opt. Express **16,** 7641 (2008).
4. H. T. Chen, W. J. Padilla, M. J. Cich, A. K. Azad, R. D. Averitt, and A. J. Taylor, Nature Photonics **3,** 148 (2009).
5. D. R. Smith, W. J. Padilla, D. C. Vier, S. C. Nemat–Nasser, and S. Schultz, Phys. Rev. Lett. **84,** 4184 (2000).
6. J. Huangfu, L. Ran, H. Chen, X. Zhang, K. Chen, T. M. Grzegoczyk, and J. A. Kong, Appl. Phys. Lett. **84,** 1537 (2004).
7. H. Chen, L. Ran, J. Huangfu, X. Zhang, K. Chen, T. M. Grzegorczyk, and J. A. Kong, Phys. Rev. E **70,** 057605 (2004).
8. J. Zhou, T. Koschny, L. Zhang, G. Tuttle, and C. M. Soukoulis, Appl. Phys. Lett. **88,** 221103 (2006).
9. J. Zhou, L. Zhang, G. Tuttle, T. Koschny, and C. M. Soukoulis, Phys. Rev. B **73,** 041101 (2006).
10. M. Kafesaki, I. Tsiapa, N. Katsarakis, Th. Koschny, C. M. Soukoulis, and E. N. Economou, Phys. Rev. B **75,** 235114 (2007).
11. W. Zhu, X. Zhao, and J. Guo, Appl. Phys. Lett. **92,** 241116 (2008).
12. Y. Yuan, C. Bingham, T. Tyler, S. Palit, T. H. Hand, W. J. Padilla, D. R. Smith, N. M. Jokerst, and S. A. Cummer, Opt. Express **16,** 9746 (2008).
13. D. R. Smith, S. Schultz, P. Markos, and C. M. Soukoulis, Phys. Rev. B **65,** 195104 (2002).
14. D. R. Smith, D. C. Vier, Th. Koschny, and C. M. Soukoulis, Phys. Rev. E **71,** 036617 (2005).
15. S. Zhang, W. Fan, N. C. Panoiu, K. J. Malloy, R. M. Osgood, and S. R. J. Brueck, Phys. Rev. Lett. **95,** 137404 (2005).
16. J. B. Pendry, A. J. Holden, W. J. Stewart, and I. Youngs, Phys. Rev. Lett. **76,** 4773 (1996).